

An approach for electrical self-stabilization of high-temperature superconducting wires for power applications

T. Aytug,^{a)} M. Paranthaman, H. Y. Zhai, A. A. Gapud, K. J. Leonard, P. M. Martin, A. Goyal, J. R. Thompson,^{a)} and D. K. Christen
Oak Ridge National Laboratory, Oak Ridge, Tennessee 37831

(Received 7 May 2004; accepted 16 July 2004)

Electrical and thermal stability of high-temperature superconducting (HTS) wires/tapes are essential in applications involving efficient production, distribution, and storage of electrical energy. We have developed a conductive buffer layer structure composed of bilayer $\text{La}_{0.7}\text{Sr}_{0.3}\text{MnO}_3/\text{Ir}$ on a textured Ni–W alloy metal tape to functionally shunt the HTS layer to the underlying substrate. The key feature is the Ir layer, which serves as a barrier to both inward diffusion of oxygen and outward diffusion of metal substrate cations during fabrication. Electrical and microstructural property characterizations of $\text{YBa}_2\text{Cu}_3\text{O}_{7-\delta}$ films on short prototype conductors demonstrate self-field critical current density values, J_c , exceeding $2 \times 10^6 \text{ A/cm}^2$ at 77 K and excellent electrical coupling to the underlying metal substrate, with no unwanted insulating oxide interfaces. Implementing this approach in power technologies would significantly increase the engineering current density of the conductor and reduce overall process costs. © 2004 American Institute of Physics.

[DOI: 10.1063/1.1794848]

The conduction of electric currents in the absence of electrical resistivity at cryogenic temperatures (30–77 K) offers significant potential for high temperature superconductors (HTS) in many energy efficient applications. Usage of HTS wires/tapes (coated conductors) in electric power systems could greatly reduce energy losses and significantly increase electric efficiency and stability across a gamut of electricity delivery and utilization. In general, coated conductor architectures involve epitaxial deposition of a thin layer (1–2 μm) of HTS film [usually $\text{YBa}_2\text{Cu}_3\text{O}_{7-\delta}$ (YBCO)] on biaxially textured buffer layers deposited on a 50- μm -thick flexible metal substrate.¹ For effective implementation, it is necessary to electrically and thermally stabilize the HTS coating by means of a parallel electrical conduction path capable of shunting the current away from the HTS layer in the event of a local transient to the dissipative state (possibly caused by a thermal spike, a micro-crack in the superconductor layer, or by a current surge beyond the superconductor's critical current, I_c .^{2–5} Otherwise, because of the extremely high current density, J , carried by the superconductor layer ($\sim 10^6 \text{ A/cm}^2$), such an event would immediately damage an electrically isolated superconducting coating due to the extreme level of local Joule heating.

From an applications perspective, the optimum engineering current density, J_E (current per unit total cross-sectional area), is achieved by using the metal tape as both substrate and stabilizer. Such a configuration requires electrical connectivity between the HTS layer and the underlying metal substrate by use of an intermediate conductive buffer layer structure.^{2,6} On the other hand, if the substrate tape has high resistivity ($>10 \mu\Omega \text{ cm}$ at 77 K) or the buffer layers are insulating, an additional thick high conductivity metal stabilizer layer (e.g., Cu or Ag) must be added onto the HTS coating.^{3,5} Presently, all pre-commercial approaches to coated conductors use low-conductivity Ni-alloy tapes and

insulating buffer layers, so that an additional layer of copper is laminated onto the superconductor.⁵ An envisioned HTS wire architecture would involve the combined use of a strong, high conductivity Cu-alloy tape substrate and a conductive buffer layer, thereby eliminating the need for additional stabilizing layers. This achievement would not only yield substantial improvement in J_E , but also would provide benefits in reduced material cost, absence of substrate ferromagnetism, and increased thermal conductivity when compared to Ni alloys.

In our previous investigations on the development of conductive buffer layers directly on pure Cu or Ni surfaces, electrical connectivity proved to be a major challenge, mainly because of the poor oxidation resistance and high reactivity/diffusivity of Cu or Ni.^{2,6–8} A discontinuous insulating oxide layer (i.e., Cu_2O or NiO) usually forms at the metal/substrate interface either during the growth of conductive buffer layers or through the processing of YBCO films. In this study, we have addressed these issues by using several properties of the fcc metal Ir as a base buffer, followed by a single buffer layer of $\text{La}_{0.7}\text{Sr}_{0.3}\text{MnO}_3$ (LSMO). This buffer layer combination improves oxidation resistance of the substrate and effectively blocks diffusion of the substrate species into the HTS layer. Iridium is identified as having excellent oxidation and corrosion resistance among platinum group metals,⁹ and low oxygen diffusivity.¹⁰ Moreover, its native oxide, IrO_2 , under conditions of stability, is characterized by metallic conductivity (bulk resistivity, $\rho \sim 30\text{--}100 \mu\Omega \text{ cm}$) and chemical inertness.^{10–12} These properties make Ir a candidate for a conductive interface, while LSMO is selected for its electrical conductivity and structural/chemical compatibility with YBCO.^{6–8} In this work, we have used Ni-alloy substrates for a proof-of-principle assessment of the feasibility of LSMO/Ir as a conductive buffer interface.

Magnetron sputtering systems with rf and dc sources were used to deposit LSMO and Ir thin films, respectively, on biaxially textured Ni-3 at. % W (Ni–W) substrates. For Ir film growth, sputtering gas of Ar+4% H_2 and substrate tem-

^{a)}Also at: Department of Physics, University of Tennessee, Knoxville, TN 37996; electronic mail: aytugt@ornl.gov

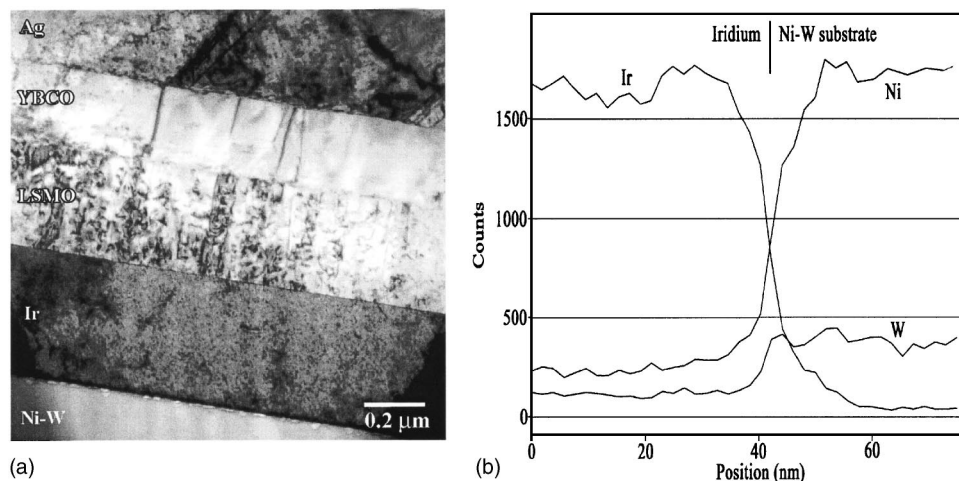


FIG. 1. (a) Cross-section TEM bright-field image of the 0.2- μm -thick YBCO/LSMO/Ir/Ni(W) composite structure showing well-defined interfaces between the layers. (b) High-resolution EDS line scan across the Ir/Ni-W boundary showing undetectable oxygen levels and sharp drop of Ni and W signal at the interface.

peratures in the range of 550–650 °C were used. Subsequent LSMO deposition was conducted at 625–700 °C in a mixture of forming gas and 5×10^{-5} Torr of H_2O . For both films, sputter-gas pressure was around 10 mTorr. Film thicknesses were varied from 50 to 500 nm for Ir and from 40 to 300 nm for LSMO. YBCO films with thickness in the range of 200–1500 nm were grown by pulsed laser deposition, using a KrF excimer laser system operated at an energy density of $\approx 2 \text{ J/cm}^2$. Samples were characterized for crystal structure, phase, and texture by x-ray diffraction (XRD). Cross-section examinations of the samples were conducted by a high-resolution transmission electron microscope (TEM) equipped with energy dispersive spectrometry (EDS) unit. A standard four-probe technique was used to evaluate the electrical properties, including the temperature-dependent resistivity of the conductive buffer layers, superconducting transition temperature (T_c), critical current density (J_c), and current-voltage (I - V) characteristics of the composite structure. Values of J_c were assigned at a $1 \mu\text{V/cm}$ criterion.

Typical XRD spectra of YBCO films deposited on LSMO/Ir/Ni-W show all diffraction peaks are (00 l) type reflections, indicating c -axis growth for each layer. For a 0.2 μm thick YBCO film sample, the XRD out-of-plane ($\Delta\omega$) FWHM (full width at half maximum) widths for YBCO(006), LSMO(002), Ir(002) and Ni-W(002) are 4.7°, 4.6°, 5.2°, and 5.3°, respectively. The in-plane ($\Delta\phi$) scans on the (111) peak reflections for LSMO, Ir and Ni-W, and on the (103) reflection for YBCO yielded FWHM values of 7.2°, 7.7°, 7.7°, and 8°, respectively. After 1- μm -thick YBCO deposition, there is no evidence of peaks from unwanted insulating NiO or other reactants. This is a significant observation in view of our previous conductive buffer-layer studies on Ni-based templates, which always showed some NiO formation at the substrate/buffer-layer interface, even after growth of only 0.2- μm -thick YBCO. The interfaces between the various layers in a 0.2- μm -thick YBCO/LSMO/Ir/Ni-W sample were examined by high resolution TEM. An image of the thinned cross-sectional area of the sample is shown in Fig. 1. To clearly identify the interfaces, the sample was tilted away from the [010] Ni-W zone axis along the (001) direction. All interfaces are clean and homogeneous with no intermediate reaction zones or phases present between the individual layers. More important, an EDS line scan (using an electron probe approximately 1.5 nm diameter) across the boundary between the Ir

buffer and Ni-W substrate [Fig. 1(b)] confirmed the absence of oxygen within the Ir, Ni-W, or at the interface. Sharp changes of the Ir, Ni, and W signals at the interface also verify that there is no significant intermixing. However, note that compared to present YBCO conditions, it is possible that elevated temperatures and longer YBCO processing times may lead to Ir-Ni interdiffusion. The details of this issue are currently under investigation. While Ir has equiaxed grain structure, both YBCO and LSMO exhibit c -axis columnar growth, typical for perovskites, with no secondary phases or porosity. Imaging under the tilted off zone conditions some porosity is visible at the Ir and Ni-W boundary, although diffraction and high-resolution imaging confirmed that the interface is atomically coherent. There is no indication of possible reaction phases that could have been pulled out during the sample preparation. Possibly, the pores result from strain induced by either lattice-mismatch or the large difference in thermal expansion coefficient between the Ir layer and the substrate.

The XRD and TEM observations are consistent with measurements of the temperature-dependent resistivity, $\rho_{\text{net}}-T$ (Fig. 2). Here ρ_{net} is calculated from the thickness of the entire structure assuming a negligible interfacial contact resistance (i.e., $< 10^{-8} \Omega \text{ cm}^2$). For direct comparison, data for

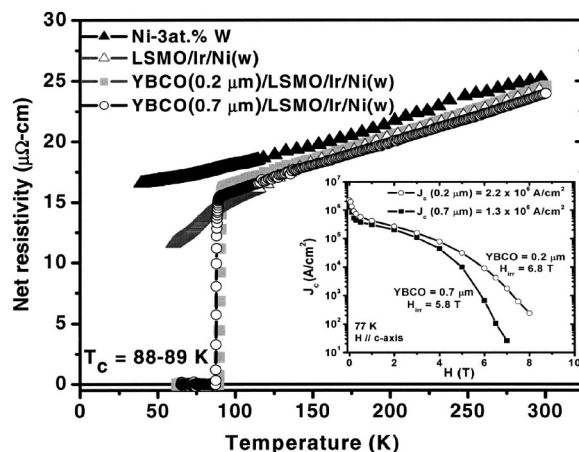


FIG. 2. Temperature-dependent net resistivity measurements for 0.2- and 0.7- μm thick-YBCO samples grown on conductive LSMO/Ir/Ni-W substrates. For comparison, data for LSMO/Ir/Ni-W and biaxially textured Ni-W substrate are also included. Inset shows the field-dependent transport critical current densities at 77 K for the same YBCO films.

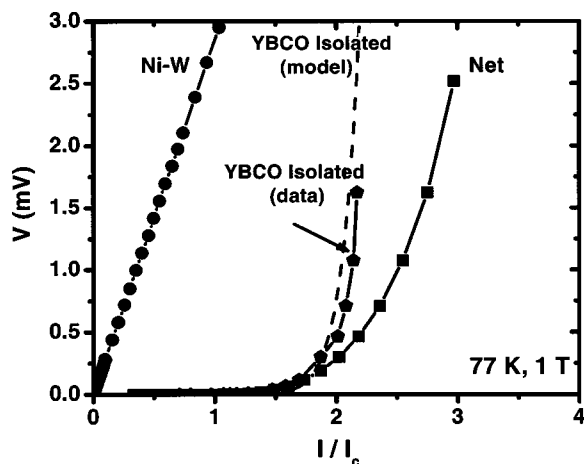


FIG. 3. The I - V curves obtained from the 0.2- μm -thick YBCO on conductive LSMO/Ir/Ni-W in a field of 1 T and for the bare Ni-W substrate. Also included are a model curve with power law $n=15$ and the curve derived for the isolated YBCO film from the actual measurement.

bare Ni-W substrate are also included. The metallic $\rho_{\text{net}}-T$ behavior of the as-deposited conductive LSMO/Ir/Ni-W is indistinguishable from the same structure after deposition of a thick (0.7 μm) YBCO layer. This observation indicates excellent electrical coupling between YBCO-LSMO-Ir-(Ni-W). The presence of a native metal oxide layer at the substrate/buffer interface would likely decouple the HTS layer, which in turn would increase the calculated ρ_{net} of the YBCO/LSMO/Ir/Ni-W by nearly a factor of 300 times the present value. The comparable T_c values, in the range of 88–89 K for both the 0.2- and 0.7- μm -thick YBCO films further point to the effectiveness of Ir layers as diffusion barriers to Ni and W, since growing thicker films requires longer time at elevated temperatures in the presence of an oxygen ambient. The slightly lower net normal state resistivity for the Ir coated architectures as compared to that of the Ni-W substrate, along with the sharp decrease observed in ρ_{net} at lower temperatures (<100 K), is associated with the much lower resistivity [$\rho(300\text{ K})=4.8\ \mu\Omega\text{ cm}$] and larger resistivity ratio of Ir [$\rho(300\text{ K})/\rho(77\text{ K})$], compared to Ni-W. The inset of Fig. 2 shows the transport J_c at 77 K for the same YBCO films as a function of magnetic field, applied parallel to c axis. Self-field J_c values of 2.2 and 1.3 were obtained for the 0.2 and 0.7 μm YBCO coatings, respectively. These high values of J_c result from the presence of only low-angle grain-to-grain alignments, along with an overall high quality YBCO coating, free of cation contamination. However, the decrease of J_c with increasing YBCO thickness is probably associated with degradation in the microstructure and crystalline orientation of PLD films, as is well documented.^{13,14}

To evaluate the stability provided by the conductive buffer interface, we measured current versus voltage (I - V) characteristics of YBCO/LSMO/Ir/Ni-W. Tests were conducted on 0.2- μm -thick YBCO films at an applied field of 1 T due to the limitations of our current source. In Fig. 3 are displayed three I - V curves: for the Ni-W tape only; for a typical isolated HTS coating at 77 K, 1 T having a power law relation $V \propto (I/I_c)^n$ with $n=15$; and the I - V for the actual sample. The data from the sample agree well with the expected I - V curve for the net, combined ideal case of nonlinear HTS layer and ohmic LSMO/Ir/Ni-W. That is, for an

envisioned current surge with $I > I_c$, the total current is partitioned ideally between the YBCO and the substrate [i.e. $I_{\text{Total}} = I_{\text{Substrate}} + I_{\text{HTS}} = V/R_{\text{Substrate}} + I_c(V/V_c)^{1/n}$] via the conductive interface, where V_c is the voltage criterion to deduce I_c . As a check, we are able to recover the I - V behavior of an isolated HTS film by subtracting the expected current through the substrate from the total measured current. The result of this exercise, labeled “model” in Fig. 3, is in reasonable agreement with the curve generated from the expected power law relation. Although for the present case of a thin YBCO coating in a magnetic field, electrical stability to an over-current of $\sim 3 I_c$ is provided, the ρ_{net} value of $\sim 16\ \mu\Omega\text{ cm}$ is not sufficiently low to provide necessary stabilization for a practical, high-current conductor. As an example, for a YBCO film carrying 100 A/cm width (a practical current level), in the event of a transient loss of superconductivity, the dissipated heat flux would be $\sim 32\text{ W/cm}^2$, which is above the critical heat flux of $\sim 10\text{ W/cm}^2$ for boiling LN_2 .³ Nevertheless, the present results establish a proof-of-principle for a conductive buffer stack on a metal substrate and provide motivation for the development of a fully conductive Cu-based RABiTS (rolling assisted biaxially textured substrates), where the metal substrate conductivity is sufficient to provide stabilization. Research is in progress on both the development of textured copper-based substrates and implementation of the Ir-based architecture, which promises high electrical conduction to the substrate combined with an excellent barrier to both oxygen and cation diffusion.

This work was supported by the U.S. Department of Energy, Office of Electric Transmission and Distribution. The research was performed at the Oak Ridge National Laboratory, managed by U.T.-Battelle, LLC for the USDOE under Contract No. DE-AC05-00OR22725.

¹A. Goyal, D. P. Norton, J. D. Budai, M. Paranthaman, E. D. Specht, D. M. Kroeger, D. K. Christen, Q. He, B. Saffian, F. A. List, D. F. Lee, P. M. Martin, C. E. Klabunde, E. Hatfield, and V. K. Sikka, Appl. Phys. Lett. **69**, 1795 (1996).

²T. Aytug, B. W. Kang, C. Cantoni, E. D. Specht, M. Paranthaman, A. Goyal, D. T. Verebelyi, D. K. Christen, J. Z. Wu, R. E. Ericson, C. L. Thomas, C.-Y. Yang, and S. E. Babcock, J. Mater. Res. **16**, 2661 (2001).

³C. Cantoni, T. Aytug, D. T. Verebelyi, M. Paranthaman, E. D. Specht, D. P. Norton, and D. K. Christen, IEEE Trans. Appl. Supercond. **11**, 3309 (2001).

⁴Y. Fu, O. Tsukamoto, and M. Furuse, IEEE Trans. Appl. Supercond. **13**, 1780 (2003).

⁵D. Verebelyi, E. Harley, J. Scudiere, A. Otto, U. Schoop, C. Theime, M. Rupich, and A. Malozemoff, Supercond. Sci. Technol. **16**, 1158 (2003).

⁶T. Aytug, M. Paranthaman, B. W. Kang, S. Sathyamurthy, A. Goyal, and D. K. Christen, Appl. Phys. Lett. **79**, 2205 (2001).

⁷T. Aytug, M. Paranthaman, J. R. Thompson, A. Goyal, N. Rutter, H. Y. Zhai, A. A. Gapud, A. O. Ijaluola, and D. K. Christen, Appl. Phys. Lett. **83**, 3963 (2003).

⁸M. P. Paranthaman, T. Aytug, and D. K. Christen, U.S. Patent No. 6,617,283 (2003).

⁹H. Jehn, J. Less-Common Met. **100**, 321 (1984).

¹⁰C. U. Pinnow, I. Kasko, N. Nagel, T. Mikolajick, C. Dehm, F. Jahnel, M. Seibt, U. Geyer, and K. Samwer, J. Appl. Phys. **91**, 1707 (2002).

¹¹C. U. Pinnow, I. Kasko, C. Dehm, B. Jobst, M. Seibt, and U. Geyer, J. Vac. Sci. Technol. B **19**, 1857 (2001).

¹²T. Nakamura, Y. Nakao, A. Kamisawa, and H. Takasu, Appl. Phys. Lett. **65**, 1522 (1994).

¹³S. R. Foltyn, P. Tiwari, R. C. Dye, M. Q. Le, and X. D. Wu, Appl. Phys. Lett. **63**, 1848 (1993).

¹⁴S. R. Foltyn, Q. X. Jia, P. N. Arendt, L. Kinder, Y. Fan, and J. F. Smith, Appl. Phys. Lett. **75**, 3692 (1999).